AIAA JOURNAL
Vol. 44, No. 9, September 2006

Nonlinear Damped Vibrations of a Laminated Composite Plate Subjected to Blast Load

Zafer Kazancı*
Turkish Air Force Academy, Yesilyurt, 34149 İstanbul, Turkey
and
Zahit Mecitoğlu†
İstanbul Technical University, Maslak, 34469 İstanbul, Turkey

DOI: 10.2514/1.17620

This research deals with the derivation and solution of nonlinear dynamic equations of a clamped laminated plate exposed to blast load including structural damping effects. Dynamic equations of the plate are derived by the use of the virtual work principle. The geometric nonlinearity effects are taken into account with the von Kármán large deflection theory of thin plates. An appropriate approximate solution is assumed for the space domain considering the finite element analysis results for the large deformation static analysis of the laminated plate. The Galerkin method is used to obtain the nonlinear differential equations in the time domain. These nonlinear differential equations include structural damping effects. The finite difference method is applied to solve the system of coupled nonlinear equations. The results of the theoretical analysis are compared with the experimental results. Good agreement is found for the peak values and frequencies. Effects of aspect ratio and damping on the dynamic response of the plate are examined. The damping coefficient greatly affects the nonlinear dynamic response.

Nomenclature

a, b	=	dimensions of the plate
d_1, d_2, d_3	=	viscous damping coefficients
E_1, E_2	=	Young's moduli
G_{12}	=	shear modulus
h	=	plate thickness
h_k	=	kth ply thickness
M_x, M_y, M_{xy}	=	moment components
$\bar{m}$	=	unit area mass of plate
N_x, N_y, N_{xy}	=	force components
P	=	blast pressure
p_m	=	peak pressure
$\bar{Q}_{ij}$	=	elastic constant components for a laminated composite ($i = 1, 2, 6$; $j = 1, 2, 6$)
q_x, q_y, q_z	=	load vectors
t	=	time
t_p	=	positive phase duration
U, V, W	=	time-dependent parts of displacement components
u, v, w	=	displacement components in the x, y, z directions
u^0, v^0, w^0	=	displacement components of reference surface in the x, y, z directions
$\dot{u}, \dot{v}, \dot{w}$	=	components of velocity vector
$\ddot{u}, \ddot{v}, \ddot{w}$	=	components of acceleration vector
α	=	waveform parameter
$\varepsilon_x, \varepsilon_y, \varepsilon_{xy}$	=	strain components
$\varepsilon_x^0, \varepsilon_y^0, \varepsilon_{xy}^0$	=	membrane strain components
ζ	=	damping ratio
$\kappa_x, \kappa_y, \kappa_{xy}$	=	plate curvatures
ν_{12}	=	Poisson's ratio
ρ	=	density of material
$\sigma_x, \sigma_y, \sigma_{xy}$	=	stress components
ω	=	fundamental frequency

I. Introduction

ADVANCED laminated composites are used in several engineering fields such as space station structures, aircrafts, automobiles, and submarines. The increased use of advanced new composite material structures implies a necessity to reconsider the problem of nonlinear dynamic behavior of laminated composite plates exposed to time-dependent pulses, such as sonic boom and blast loadings.

A number of studies have been performed concerning the nonlinear analysis of plates. Leissa [1] has addressed numerous studies on the theory of the vibration of plates in his book. A comprehensive list of papers published in the area is given in Reddy [2,3].

Türkmen and Mecitoğlu [4,5] have performed some experimental and approximate-numerical studies on the nonlinear structural response of laminated composites subjected to blast load. Türkmen [6] has compared experimental and theoretical methods. Nosier et al. [7] have investigated the motion of viscously damped laminated composite flat panels. Librescu et al. [8] have addressed the problem of the dynamic response of sandwich panels exposed to blast loadings. Kazancı et al. [9] have considered in-plane stiffness and inertias in the analytical solution of the laminated composite plate under the blast load. Present work includes the structural damping effects as well as in-plane stiffness and inertia effects on the motion of a laminated composite plate under blast load.

In this study, the equations of motion of the laminated composite rectangular plate subjected to the blast load are derived in the frame of the von Kármán large deflection theory of thin plates. The clamped boundary conditions are assumed for all edges of the plate. The equations of motion are derived using the virtual work principle. The structural viscous damping developed by Rayleigh [10] is taken into account in the derivation of the equations. The displacement field in the space domain is approximated by the appropriate functions, which satisfy the certain boundary and symmetry/antisymmetry conditions. For this purpose the laminated composite plate is discretized by the laminated shell element of ANSYS 10.0 software and a static analysis is performed considering large deformations and geometric nonlinearities. Then, the Galerkin method is applied on the equations of motion to obtain a set of nonlinear-coupled equations in

Presented as Paper 2339 at the 46th AIAA/ASME/ASCE/AHS/ASC Structures, Structural Dynamics, and Materials Conference, Hyatt Regency Austin, Austin, Texas, 18–21 April 2005; received 11 May 2005; revision received 18 March 2006; accepted for publication 31 March 2006.

*Ph.D. Student, Capt., Aeronautical Engineering Department.
†Professor, Faculty of Aeronautics and Astronautics.

time domain. The resulting equations are solved using a finite difference technique. The displacement variation with time is obtained for the centroid of the plate and compared with the experimental results. Good agreement is obtained for the peak values of response and the frequencies of the vibrations. Effects of the aspect ratio and damping parameter are also studied. The damping coefficient greatly affects the nonlinear dynamic response.

II. Equations of Motion

In this section, a mathematical model for the laminated composite plate subjected to blast load is presented. The rectangular plate with length a, width b, and thickness h is depicted in Fig. 1. The Cartesian axes are used in the derivation.

The following approximation theorem of Weierstrass [11] holds: "*Any function which is continuous in an interval may be approximated uniformly by polynomials in this interval.*" Thus, the displacement field in the plate can be represented by the following relationships:

$$\begin{aligned} u(x,y,z,t) &= u^0(x,y,t) + z\alpha_1^0(x,y,t) + z^2\alpha_2^0(x,y,t) + \cdots \\ v(x,y,z,t) &= v^0(x,y,t) + z\beta_1^0(x,y,t) + z^2\beta_2^0(x,y,t) + \cdots \\ w(x,y,z,t) &= w^0(x,y,t) + z\gamma_1^0(x,y,t) + z^2\gamma_2^0(x,y,t) + \cdots \end{aligned} \quad (1)$$

The Kirchhoff–Love hypothesis for linear elastic thin plates results in the linearly distributed tangential displacements and a constant normal displacement through the thickness of the plate, and hence Eq. (1) is simplified as follows:

$$\begin{aligned} u(x,y,z,t) &= u^0(x,y,t) - z\alpha_1^0(x,y,t) \\ v(x,y,z,t) &= v^0(x,y,t) - z\beta_1^0(x,y,t) \\ w(x,y,z,t) &= w^0(x,y,t) \end{aligned} \quad (2)$$

where α_1^0 and β_1^0 are the rotations of the normal to the middle surface during deformation about the x and y axes, respectively, and can be written as

$$\alpha_1^0 = \frac{\partial w^0(x,y,t)}{\partial x}, \qquad \beta_1^0 = \frac{\partial w^0(x,y,t)}{\partial y} \quad (3)$$

In Eqs. (1–3) the superscript zero $()^0$ indicates the displacement components of the reference surface.

The strain-displacement relations for the von Kármán plate can be written as

$$\varepsilon_x = \varepsilon_x^0 + z\kappa_x, \qquad \varepsilon_y = \varepsilon_y^0 + z\kappa_y, \qquad \varepsilon_{xy} = \varepsilon_{xy}^0 + z\kappa_{xy} \quad (4)$$

where ε_x^0, ε_y^0, and ε_{xy}^0 and κ_x, κ_y, and κ_{xy} are given by

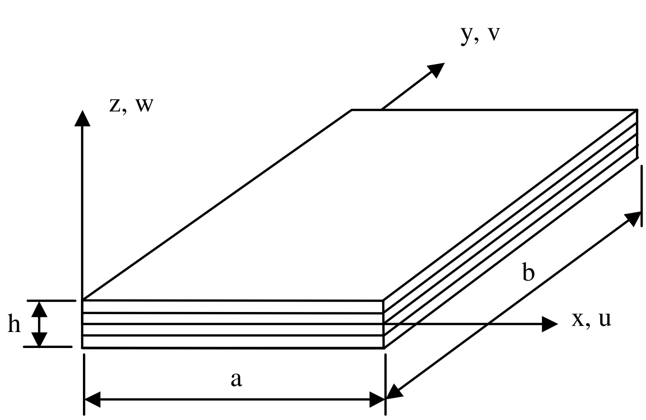

Fig. 1 Laminated plate and coordinate system.

$$\begin{aligned} \varepsilon_x^0 &= \frac{\partial u^0}{\partial x} + \frac{1}{2}\left(\frac{\partial w^0}{\partial x}\right)^2, & \kappa_x &= -\frac{\partial^2 w^0}{\partial x^2} \\ \varepsilon_y^0 &= \frac{\partial v^0}{\partial y} + \frac{1}{2}\left(\frac{\partial w^0}{\partial y}\right)^2, & \kappa_y &= -\frac{\partial^2 w^0}{\partial y^2} \\ \varepsilon_{xy}^0 &= \frac{\partial u^0}{\partial y} + \frac{\partial v^0}{\partial x} + \frac{\partial w^0}{\partial x}\frac{\partial w^0}{\partial y}, & \kappa_{xy} &= -2\frac{\partial^2 w^0}{\partial x \partial y} \end{aligned}$$

The effective elastic constants are used for defining the constitutive model of the laminated composite. The constitutive equations can be expressed as

$$\begin{bmatrix} \sigma_x \\ \sigma_y \\ \sigma_{xy} \end{bmatrix} = \begin{bmatrix} \bar{Q}_{11} & \bar{Q}_{12} & \bar{Q}_{16} \\ \bar{Q}_{12} & \bar{Q}_{22} & \bar{Q}_{26} \\ \bar{Q}_{16} & \bar{Q}_{26} & \bar{Q}_{66} \end{bmatrix} \begin{bmatrix} \varepsilon_x \\ \varepsilon_y \\ \varepsilon_{xy} \end{bmatrix} \quad (5)$$

Force and moment components of the plate can be written as

$$\begin{Bmatrix} \{N\} \\ \{M\} \end{Bmatrix} = \begin{bmatrix} [A] & [B] \\ [B] & [D] \end{bmatrix} \begin{Bmatrix} \{\varepsilon^0\} \\ \{\kappa\} \end{Bmatrix} \quad (6)$$

The coefficients in the matrices are given as follows:

$$\begin{aligned} A_{ij} &= \sum_{k=1}^{n} (\bar{Q}_{ij})_k (h_k - h_{k-1}), \\ B_{ij} &= 1/2 \sum_{k=1}^{n} (\bar{Q}_{ij})_k (h_k^2 - h_{k-1}^2) \\ D_{ij} &= 1/3 \sum_{k=1}^{n} (\bar{Q}_{ij})_k (h_k^3 - h_{k-1}^3) \end{aligned}$$

$\{N\}$ and $\{M\}$ in Eq. (6) are the vectors of force and moment components and are given by

$$\{N\} = \begin{Bmatrix} N_x \\ N_y \\ N_{xy} \end{Bmatrix} \qquad \{M\} = \begin{Bmatrix} M_x \\ M_y \\ M_{xy} \end{Bmatrix}$$

If the blast source is distant enough from the plate, the blast pressure can be described in terms of the Friedlander exponential decay equation as [12]

$$P(t) = p_m(1 - t/t_p)e^{-\alpha t/t_p} \quad (7)$$

where the negative phase of the blast is included.

Using the constitutive equations and the strain-displacement relations in the virtual work and applying the variational principles, nonlinear dynamic equations of a laminated composite plate can be obtained in terms of midplane displacements as follows:

$$\begin{aligned} & L_{11}u^0 + L_{12}v^0 + L_{13}w^0 + N_1(w^0) + d_1\dot{u}^0 + \bar{m}\ddot{u}^0 - q_x = 0 \\ & L_{21}u^0 + L_{22}v^0 + L_{23}w^0 + N_2(w^0) + d_2\dot{v}^0 + \bar{m}\ddot{v}^0 - q_y = 0 \\ & L_{31}u^0 + L_{32}v^0 + L_{33}w^0 + N_3(u^0, v^0, w^0) + d_3\dot{w}^0 \\ & \quad + \bar{m}\ddot{w}^0 - q_z = 0 \end{aligned} \quad (8)$$

including structural damping where L_{ij} and N_i are linear and nonlinear operators. The explicit expressions of the operators can be found in the Appendix. The boundary conditions are

$$
\begin{aligned}
&u^0(0,y,t) = u^0(a,y,t) = u^0(x,0,t) = u^0(x,b,t) = 0\\
&\frac{\partial u^0}{\partial x}(0,y,t) = \frac{\partial u^0}{\partial x}(a,y,t) = \frac{\partial u^0}{\partial y}(x,0,t) = \frac{\partial u^0}{\partial y}(x,b,t) = 0\\
&v^0(0,y,t) = v^0(a,y,t) = v^0(x,0,t) = v^0(x,b,t) = 0\\
&\frac{\partial v^0}{\partial x}(0,y,t) = \frac{\partial v^0}{\partial x}(a,y,t) = \frac{\partial v^0}{\partial y}(x,0,t) = \frac{\partial v^0}{\partial y}(x,b,t) = 0\\
&w^0(0,y,t) = w^0(a,y,t) = w^0(x,0,t) = w^0(x,b,t) = 0\\
&\frac{\partial w^0}{\partial x}(0,y,t) = \frac{\partial w^0}{\partial x}(a,y,t) = \frac{\partial w^0}{\partial y}(x,0,t) = \frac{\partial w^0}{\partial y}(x,b,t) = 0
\end{aligned}
$$

and initial conditions are given by

$$
\begin{aligned}
&u^0(x,y,0) = 0, \qquad v^0(x,y,0) = 0, \qquad w^0(x,y,0) = 0\\
&\dot{u}^0(x,y,0) = 0, \qquad \dot{v}^0(x,y,0) = 0, \qquad \dot{w}^0(x,y,0) = 0
\end{aligned}
$$

III. Solution Method

As mentioned by Strang [13], choosing the approximation functions is a crucial point. In this study the displacement functions are chosen by considering the results of static large deformation analysis of laminated composite by using ANSYS 10.0 software. The plate is discretized by using the eight-node laminated shell elements (SHELL 91) with eight nodes which have geometric nonlinear capability.

Figures 2–4 show the variations of $u(x)$, $v(x)$, and $w(x)$, respectively. While the $y = b/2$ line on the plate is considered for the variations of $u(x)$ and $w(x)$, the $y = b/4$ line on the plate is taken for the variation of $v(x)$. Figures 2–4 also include the variations of the first term of approximation functions given in Eq. (1).

It can be seen from the figures that the displacement functions for the clamped boundary conditions can be assumed in the following form appropriately:

$$
\begin{aligned}
u^0 &= \sum_{m=1}^{M}\sum_{n=1}^{N} U_{mn}(t) x^{2m}(x-a)^{2m}\left(x - \frac{a}{2}\right)^m \left(1 - \cos\frac{2n\pi y}{b}\right)\\
v^0 &= \sum_{m=1}^{M}\sum_{n=1}^{N} V_{mn}(t)\left(1 - \cos\frac{2m\pi x}{a}\right) y^{2n}(y-b)^{2n}\left(y - \frac{b}{2}\right)^n\\
w^0 &= \sum_{m=1}^{M}\sum_{n=1}^{N} W_{mn}(t)\left(1 - \cos\frac{2m\pi x}{a}\right)\left(1 - \cos\frac{2n\pi y}{b}\right)
\end{aligned}
\tag{9}
$$

Accounting only the first terms of displacement functions and applying the Galerkin method to the equations of motion given in Eq. (8), the time-dependent nonlinear differential equations are obtained

$$
\begin{aligned}
&a_0\ddot{U} + a'\dot{U} + a_1 U + a_2 V + a_3 W + a_4 W^2 + a_5 = 0\\
&b_0\ddot{V} + b'\dot{V} + b_1 V + b_2 U + b_3 W + b_4 W^2 + b_5 = 0\\
&c_0\ddot{W} + c'\dot{W} + c_1 W + c_2 W^2 + c_3 W^3 + c_4 U + c_5 V\\
&\quad + c_6 UW + c_7 VW + c_8 = 0
\end{aligned}
\tag{10}
$$

where the coefficients of the equations are given in the Appendix. The dot denotes the derivative with respect to time. The initial conditions can be expressed as

$$
\begin{aligned}
&U(0) = 0, \qquad V(0) = 0, \qquad W(0) = 0\\
&\dot{U}(0) = 0, \qquad \dot{V}(0) = 0, \qquad \dot{W}(0) = 0
\end{aligned}
$$

Nonlinear-coupled equations of motion are solved by using the finite difference method. We may arrange Eq. (10) in the matrix format,

$$
[K_0]\frac{\partial^2}{\partial t^2}\{Q\} + [K']\{T\} + [K_1]\{Q\} + [K_2]\{Q\} + [K_3] = 0 \tag{11}
$$

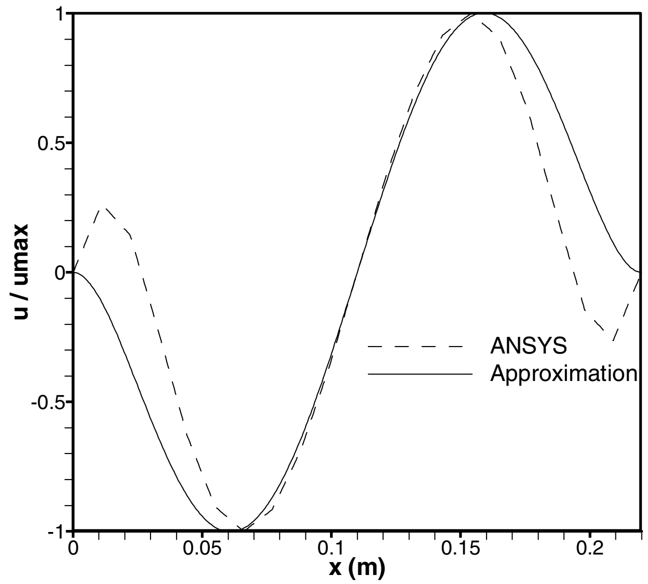

Fig. 2 Variation of $u(x)$. ($y = b/2$).

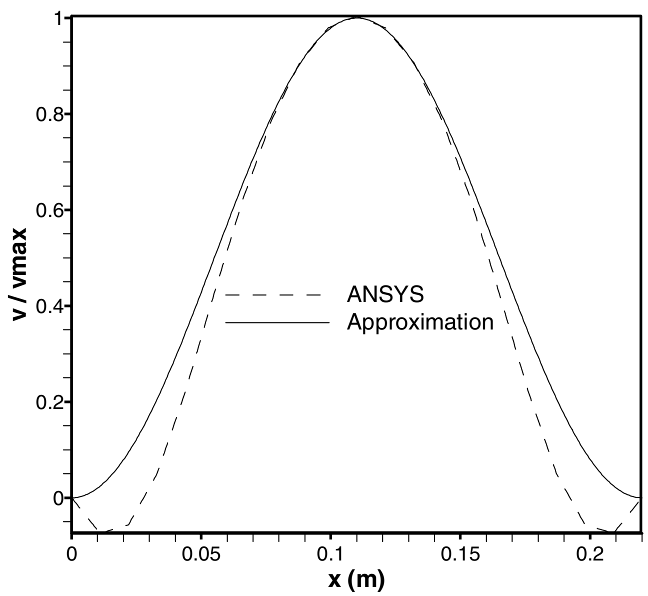

Fig. 3 Variation of $v(x)$. ($y = b/4$).

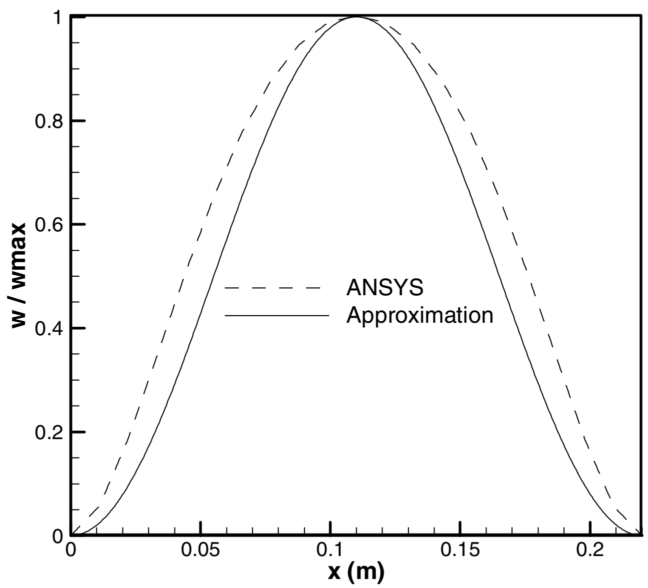

Fig. 4 Variation of $w(x)$. ($y = b/2$).

where $\{Q\} = [U\ V\ W]$ and $\{T\} = [\dot{U}\ \dot{V}\ \dot{W}\rfloor^T$. $[K_0]$, $[K']$, $[K_1]$, $[K_2]$, and $[K_3]$ matrices are defined as:

$$[K_0] = \begin{pmatrix} a_0 & 0 & 0 \\ 0 & b_0 & 0 \\ 0 & 0 & c_0 \end{pmatrix}, \qquad [K'] = \begin{pmatrix} a' & 0 & 0 \\ 0 & b' & 0 \\ 0 & 0 & c' \end{pmatrix},$$

$$[K_1] = \begin{pmatrix} a_1 & a_2 & a_3 \\ b_2 & b_1 & b_3 \\ c_4 & c_5 & c_1 \end{pmatrix}, \tag{12}$$

$$[K_2] = \begin{pmatrix} 0 & 0 & a_4 W \\ 0 & 0 & b_4 W \\ c_6 W & c_7 W & (c_2 W + c_3 W^2) \end{pmatrix}, \qquad [K_3] = \begin{bmatrix} a_5 \\ b_5 \\ c_8 \end{bmatrix}$$

If we replace the $\partial^2/\partial t^2\{Q\}$ term with $\partial/\partial t\{T\}$ in Eq. (11), we can write down

$$[K_0]\frac{\partial}{\partial t}\{T\} + [K']\{T\} + [K_4]\{Q\} + [K_3] = 0 \tag{13}$$

where $[K_4] = [K_1] + [K_2]$. Using the definition of derivation, Eq. (13) is

$$[K_0]\frac{\{T\}^{n+1} - \{T\}^n}{\Delta t} + [K']\{T\}^{n+1} + [K_4]\{Q\}^{n+1} + [K_3] = 0 \tag{14}$$

Rearranging Eq. (14) and substituting T^{n+1} with $(Q^{n+1} - Q^n)/\Delta t$, we obtain

$$\left(\frac{1}{(\Delta t)^2}[K_0] + \frac{1}{\Delta t}[K'] + [K_4]\right)\{Q\}^{n+1} = \frac{1}{\Delta t}[K_0]\{T\}^n + \left(\frac{1}{(\Delta t)^2}[K_0] + \frac{1}{\Delta t}[K']\right)\{Q\}^n - \{K_3\} \tag{15}$$

Substituting the matrices given in Eq. (12) into Eq. (15) the equations of motion are reduced into

$$\begin{aligned} A_1 U^{n+1} + A_2 V^{n+1} + A_3 W^{n+1} &= A_4 \\ B_1 U^{n+1} + B_2 V^{n+1} + B_3 W^{n+1} &= B_4 \\ C_1 U^{n+1} + C_2 V^{n+1} + C_3 W^{n+1} &= C_4 \end{aligned} \tag{16}$$

The coefficients in the equations are given in the Appendix. From Eq. (16) we obtain the following:

$$U^{n+1} = \frac{1}{A_1}[A_4 - A_2 V^{n+1} - A_3 W^{n+1}]$$

$$V^{n+1} = \frac{D_3 - D_2 W^{n+1}}{D_1} \qquad W^{n+1} = \frac{E_3 - E_4}{E_5}$$

Nonlinear terms in $[K_2]$ were linearized by iterations: In the first iteration we used W^n which is known from the previous step. After the first iteration, W^{n+1} is calculated and used in place of W^n. Iteration continues until convergence criterion is provided.

IV. Numerical Results

Türkmen and Mecitoğlu [4] have made some blast experiments using a seven-layered fiberglass fabric with (90/0 deg) fiber orientation angle for one layer, and this plate is used in the numerical analysis. Ply material properties used in the analysis and experiments are given as $E_1 = 24.14$ GPa, $E_2 = 24.14$ GPa, $G_{12} = 3.79$ GPa, $\rho = 1800$ kg/m^3, and $\nu_{12} = 0.11$. The dimensions of the plate are $a = 0.22$ m, $b = 0.22$ m, and $h = 1.96$ mm.

The experimental work [4] has shown that the pressure distribution on the plate can be taken as uniform for a distance of 1 m from the open end of the detonation tube. The blast pressure has been measured on the thick wooden plate which has the same dimensions of the laminated composite plate. A variation of blast pressure by time at the plate center is shown in Fig. 5. The parameters of the Friedlander decay equation used in the analyses are chosen as $p_m = 28.9$ kPa, $\alpha = 0.35$, and $t_p = 1.8$ ms.

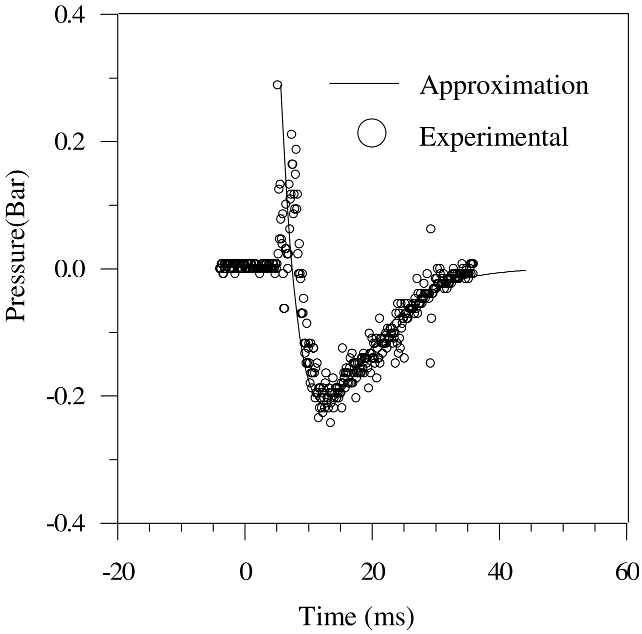

Fig. 5 Variation of blast loading by time [4].

A solution of the nonlinear-coupled equations is obtained by taking the first terms of the displacement functions. A convergence study is performed to reach the suitable time increment. A viscous damping ratio $\zeta(\equiv d_3/2\omega\bar{m})$ is taken as 0.3 for the convergence study. Here ω denotes the fundamental undamped frequency. Results of the study are shown in Fig. 6. The time increment in the subsequent analyses is taken to be 0.002 ms where the convergence criterion is ensured.

The approximate numerical and experimental results are compared in Fig. 7. The approximate numerical results are given for the two damping ratios as well as the undamped case. As shown from Fig. 7, the damping coefficient greatly affects the nonlinear dynamic response. The viscous damping decreases the vibration amplitude in a short time after the strong blast. The results of the present study show good agreement with the experimental results for the first half-cycle of motion. The agreement with the experimental results continues through the full first cycle. However, a discrepancy

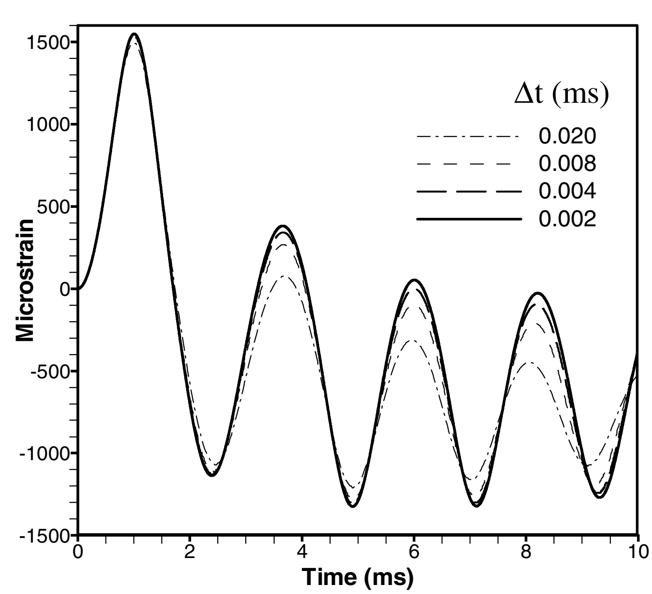

Fig. 6 Convergence of time increment.

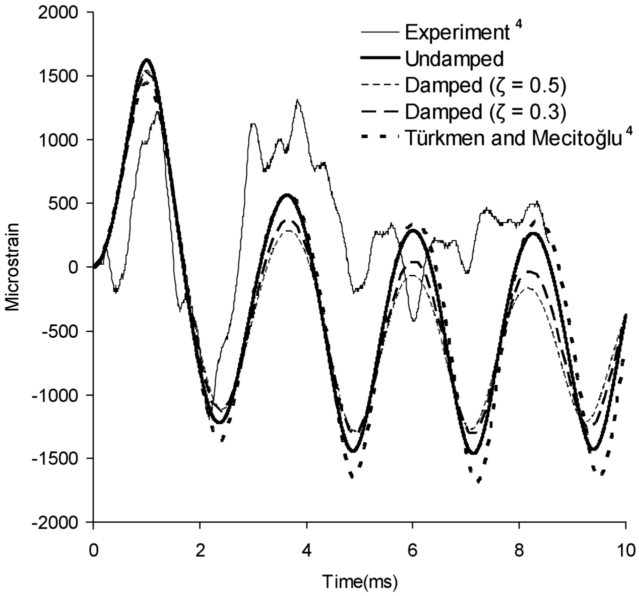

Fig. 7 Comparison of the strain-time history results.

between the theoretical and experimental results is observed after the first cycle of motion. This discrepancy would be a result of the effect of higher vibration modes on the plate response. Another source of the discrepancy would be aeroelastic interaction between the blast load and thin plate motions. In the experiments made by Türkmen and Mecitoğlu [4], while the pressure measurements are made on the thick wood samples, the strain measurements are made on the laminated thin composite plates. Hence, the results of experiments do not include the effects of blast-plate interactions.

In this study the in-plane stiffness is taken into account as a difference of the analysis made by Türkmen and Mecitoğlu [4]. The strain variation obtained in this study has a lower amplitude and closer experimental results than the approximate numerical result of Türkmen and Mecitoğlu [4], which is also presented in Fig. 7. However, the present result still shows a considerable discrepancy after the first wave.

A comparison of strain-time history results (in x direction) for the plates which have different aspect ratios is shown in Fig. 8. The results are obtained for $\zeta = 0.3$ and several aspect ratios ($a/b = 1$, 0.75, 0.5, and 0.25) by keeping the plate area constant. The analyses are performed for the seven-layered fiberglass fabric with a (90/0 deg) fiber orientation angle whose engineering material properties are given before. As a result, while the aspect ratio of the plate increases, the amplitude of the ε_x variation decreases, and the corresponding frequency increases.

The long-time displacement responses of the plate are shown in Fig. 9. The damping ratio is taken to be $\zeta = 0.3$ for the damped response analysis. The displacement response of the plate follows the blast pressure. During the time range of the strong blast effect, the

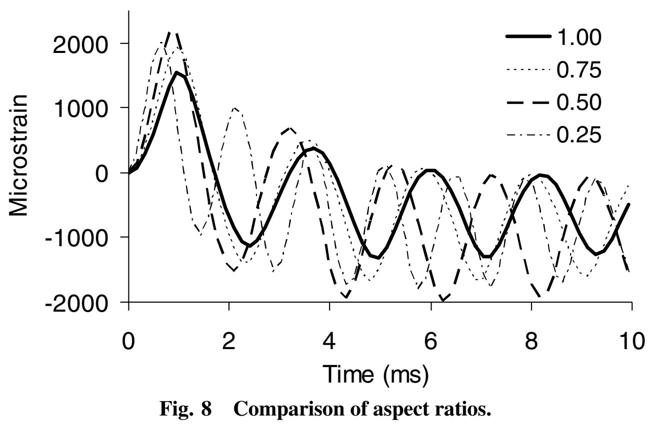

Fig. 8 Comparison of aspect ratios.

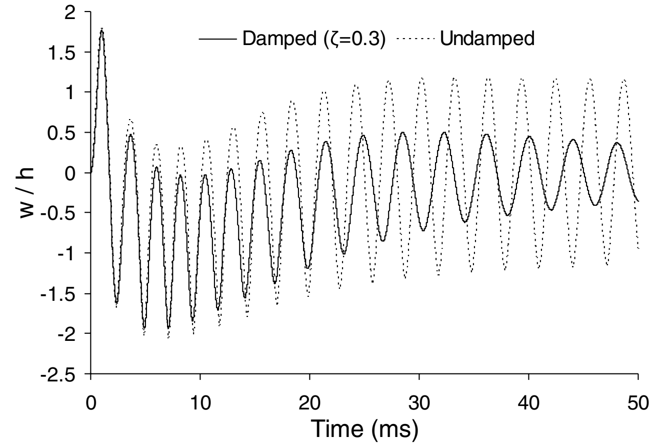

Fig. 9 Long-time response.

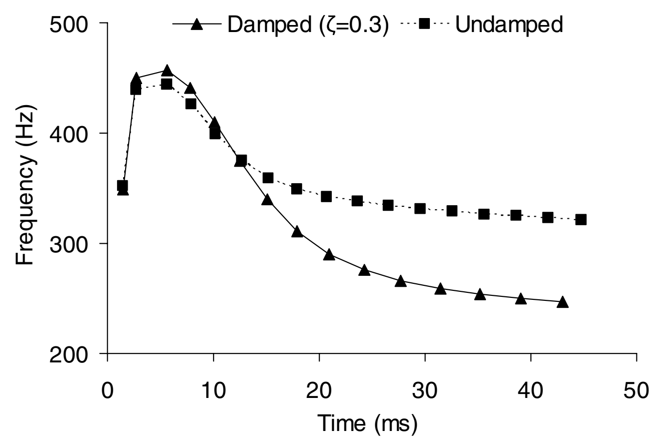

Fig. 10 Variation of frequency by time.

large deflection effects result in high in-plane tensions and therefore they increase the response frequency of the plate. After the blast, the amplitude of vibration becomes less than the plate thickness, and the response frequency tends to decrease due to the lack of the nonlinear effects. On the other hand, the frequency and amplitude of vibration decrease by the effect of structural damping.

Variation of the vibration frequency by time is shown in Fig. 10. Frequency values are obtained from the long-time displacement responses of the plate given in Fig. 9. For every wave, the inverse of the cycle time is considered for the mean frequency during the period of that wave. It can be seen from Fig. 10 that the frequency of the plate motion under the blast increases at the duration of a strong blast load because of the high nonlinearities and in-plane effects caused by large deflections. After this period the amplitude of vibration decreases and the vibration frequency also decreases. The damping effect on the vibration frequencies is pronounced in this period and it causes an additional reducing effect on the frequency.

V. Conclusion

In this study, the equations of motion of the laminated composite rectangular plate under blast load are derived in the frame of the von Kármán large deflection theory of thin plates. The Galerkin method is used to obtain a set of the nonlinear differential equations in the time domain. The nonlinear-coupled equations of the motion of the plate are solved using a finite difference method. A convergence study is performed to reach the suitable time increment for the solution.

The numerical results are correlated with the experimental results. A good agreement is found for the peak values and frequencies. Comparison of strain-time history results for the plates which have different aspect ratios is performed. The displacement response of the plate follows the blast pressure and in-plane stiffnesses affect the response frequencies in the first 20 ms that the blast pressure is quite high and they increase the response frequency of the laminated plate.

The effect of structural damping is also taken into account in this study. The damping effects decrease the vibration amplitude in a short time. It is well known that the frequency of vibration is decreased by the structural damping effects slightly. However, if the blast causes very large deflections and a consequent increase in the vibration frequency, the viscous damping effect causes a restriction on the deflections and nonlinearities and a consequent significant decrease on the vibration frequency.

The discrepancy between the experimental and theoretical results would be a result of the effect of higher vibration modes on the plate response. Another source of the discrepancy would be aeroelastic interaction between the blast load and thin plate motions.

In this study, only one term is taken for each displacement function. Therefore, the contributions of the higher modes to the structural response are not included. A study can be performed for different boundary conditions and materials. This can be the subject of future work.

Appendix

The explicit expressions of the operators:

$$L_{11} = -A_{11}\frac{\partial^2}{\partial x^2} - 2A_{16}\frac{\partial^2}{\partial x\partial y} - A_{66}\frac{\partial^2}{\partial y^2}$$

$$L_{12} = -(A_{12} + A_{66})\frac{\partial^2}{\partial x\partial y} - A_{16}\frac{\partial^2}{\partial x^2} - A_{26}\frac{\partial^2}{\partial y^2}$$

$$L_{13} = 3B_{16}\frac{\partial^3}{\partial x^2\partial y} + (B_{12} + 2B_{66})\frac{\partial^3}{\partial x\partial y^2} + B_{11}\frac{\partial^3}{\partial x^3} + B_{26}\frac{\partial^3}{\partial y^3}$$

$$L_{21} = -(A_{12} + A_{66})\frac{\partial^2}{\partial x\partial y} - A_{16}\frac{\partial^2}{\partial x^2} - A_{26}\frac{\partial^2}{\partial y^2}$$

$$L_{22} = -A_{66}\frac{\partial^2}{\partial x^2} - A_{22}\frac{\partial^2}{\partial y^2} - 2A_{26}\frac{\partial^2}{\partial x\partial y}$$

$$L_{23} = (B_{12} + 2B_{66})\frac{\partial^3}{\partial y\partial x^2} + B_{22}\frac{\partial^3}{\partial y^3} + 3B_{26}\frac{\partial^3}{\partial x\partial y^2} + B_{16}\frac{\partial^3}{\partial x^3}$$

$$L_{31} = -B_{11}\frac{\partial^3}{\partial x^3} - 3B_{16}\frac{\partial^3}{\partial x^2\partial y} - (B_{12} + 2B_{66})\frac{\partial^3}{\partial x\partial y^2} - B_{26}\frac{\partial^3}{\partial y^3}$$

$$L_{32} = -B_{16}\frac{\partial^3}{\partial x^3} - (B_{12} + 2B_{66})\frac{\partial^3}{\partial x^2\partial y} - 3B_{26}\frac{\partial^3}{\partial x\partial y^2} - B_{22}\frac{\partial^3}{\partial y^3}$$

$$L_{33} = D_{11}\frac{\partial}{\partial x^4} + 4D_{16}\frac{\partial^4}{\partial x^3\partial y} + (2D_{12} + 4D_{66})\frac{\partial^4}{\partial x^2\partial y^2} + 4D_{26}\frac{\partial^4}{\partial x\partial y^3} + D_{22}\frac{\partial^4}{\partial y^4}$$

$$N_1(w^0) = -A_{11}\frac{\partial w^0}{\partial x}\frac{\partial^2 w^0}{\partial x^2} - (A_{12} + A_{66})\frac{\partial w^0}{\partial y}\frac{\partial^2 w^0}{\partial x\partial y} - A_{16}\frac{\partial w^0}{\partial y}\frac{\partial^2 w^0}{\partial x^2} - 2A_{16}\frac{\partial w^0}{\partial x}\frac{\partial^2 w^0}{\partial x\partial y} - A_{26}\frac{\partial w^0}{\partial y}\frac{\partial^2 w^0}{\partial y^2} - A_{66}\frac{\partial w^0}{\partial x}\frac{\partial^2 w^0}{\partial y^2}$$

$$N_2(w^0) = -(A_{12} + A_{66})\frac{\partial w^0}{\partial x}\frac{\partial^2 w^0}{\partial x\partial y} - A_{22}\frac{\partial w^0}{\partial y}\frac{\partial^2 w^0}{\partial y^2} - 2A_{26}\frac{\partial w^0}{\partial y}\frac{\partial^2 w^0}{\partial x\partial y} - A_{26}\frac{\partial w^0}{\partial x}\frac{\partial^2 w^0}{\partial y^2} - A_{16}\frac{\partial w^0}{\partial x}\frac{\partial^2 w^0}{\partial x^2} - A_{66}\frac{\partial w^0}{\partial y}\frac{\partial^2 w^0}{\partial x^2}$$

$$\begin{aligned}
N_3(u^0, v^0, w^0) &= 2(B_{66} - B_{12})\left(\frac{\partial^2 w^0}{\partial x\partial y}\right)^2 \\
&+ 2(B_{12} - B_{66})\left(\frac{\partial^2 w^0}{\partial x^2}\frac{\partial^2 w^0}{\partial y^2}\right) - A_{11}\left(\frac{\partial^2 u^0}{\partial x^2}\frac{\partial w^0}{\partial x}\right) \\
&- (3A_{11}/2)\left(\frac{\partial w^0}{\partial x}\right)^2\frac{\partial^2 w^0}{\partial x^2} - (A_{12} + A_{66})\left(\frac{\partial^2 v^0}{\partial y\partial x}\frac{\partial w^0}{\partial x}\right) \\
&- 2A_{66}\left(\frac{\partial w^0}{\partial y}\frac{\partial^2 w^0}{\partial y\partial x}\frac{\partial w^0}{\partial x}\right) - 2A_{16}\left(\frac{\partial^2 u^0}{\partial y\partial x}\frac{\partial w^0}{\partial x}\right) \\
&- A_{16}\left(\frac{\partial^2 v^0}{\partial x^2}\frac{\partial w^0}{\partial x}\right) - 3A_{16}\left(\frac{\partial^2 w^0}{\partial x^2}\frac{\partial w^0}{\partial y}\frac{\partial w^0}{\partial x}\right) \\
&- 3A_{16}\left(\frac{\partial w^0}{\partial x}\right)^2\frac{\partial^2 w^0}{\partial y\partial x} - A_{26}\left(\frac{\partial^2 v^0}{\partial y^2}\frac{\partial w^0}{\partial x}\right) \\
&- 4A_{26}\left(\frac{\partial w^0}{\partial y}\frac{\partial^2 w^0}{\partial y^2}\frac{\partial w^0}{\partial x}\right) - A_{66}\left(\frac{\partial^2 u^0}{\partial y^2}\frac{\partial w^0}{\partial x}\right) \\
&- (A_{66} + A_{12}/2)\left(\frac{\partial w^0}{\partial x}\right)^2\frac{\partial^2 w^0}{\partial y^2} - (A_{12} + A_{66})\left(\frac{\partial^2 u^0}{\partial x\partial y}\frac{\partial w^0}{\partial y}\right) \\
&- A_{22}\left(\frac{\partial^2 v^0}{\partial y^2}\frac{\partial w^0}{\partial y}\right) - (3A_{22}/2)\left(\frac{\partial w^0}{\partial y}\right)^2\frac{\partial^2 w^0}{\partial y^2} \\
&- A_{26}\left(\frac{\partial^2 u^0}{\partial y^2}\frac{\partial w^0}{\partial y}\right) - 2A_{26}\left(\frac{\partial^2 v^0}{\partial x\partial y}\frac{\partial w^0}{\partial y}\right) \\
&- 3A_{26}\left(\frac{\partial^2 w^0}{\partial x\partial y}\right)\left(\frac{\partial w^0}{\partial y}\right)^2 - A_{16}\left(\frac{\partial^2 u^0}{\partial x^2}\frac{\partial w^0}{\partial y}\right) - A_{66}\left(\frac{\partial^2 v^0}{\partial x^2}\frac{\partial w^0}{\partial y}\right) \\
&- (A_{66} + A_{12}/2)\left(\frac{\partial w^0}{\partial y}\right)^2\frac{\partial^2 w^0}{\partial x^2} - A_{11}\left(\frac{\partial^2 w^0}{\partial x^2}\frac{\partial u^0}{\partial x}\right) \\
&- A_{12}\left(\frac{\partial v^0}{\partial y}\frac{\partial^2 w^0}{\partial x^2}\right) - A_{16}\left(\frac{\partial u^0}{\partial y}\frac{\partial^2 w^0}{\partial x^2}\right) - A_{16}\left(\frac{\partial v^0}{\partial x}\frac{\partial^2 w^0}{\partial x^2}\right) \\
&- A_{12}\left(\frac{\partial u^0}{\partial x}\frac{\partial^2 w^0}{\partial y^2}\right) - A_{22}\left(\frac{\partial v^0}{\partial y}\frac{\partial^2 w^0}{\partial y^2}\right) - A_{26}\left(\frac{\partial u^0}{\partial y}\frac{\partial^2 w^0}{\partial y^2}\right) \\
&- A_{26}\left(\frac{\partial v^0}{\partial x}\frac{\partial^2 w^0}{\partial y^2}\right) - 2A_{16}\left(\frac{\partial u^0}{\partial x}\frac{\partial^2 w^0}{\partial x\partial y}\right) - A_{26}\left(\frac{\partial v^0}{\partial y}\frac{\partial^2 w^0}{\partial x\partial y}\right) \\
&- 2A_{66}\left(\frac{\partial u^0}{\partial y}\frac{\partial^2 w^0}{\partial x\partial y}\right) - 2A_{66}\left(\frac{\partial v^0}{\partial x}\frac{\partial^2 w^0}{\partial x\partial y}\right)
\end{aligned}$$

Coefficients in the time-dependent nonlinear differential equations:

$$a_0 = \frac{a^{11}b}{18,480}\bar{m}, \qquad a' = \frac{a^{11}b}{18,480}d_1$$

$$a_1 = \frac{a^9(33A_{11}b^2 + a^2A_{66}\pi^2)}{13,860b}$$

$$a_2 = \frac{a^5(A_{12} + A_{66})b^5(-15 + \pi^2)^2}{4\pi^8}$$

$$a_3 = -\frac{a^3[3b^2B_{11} + a^2(B_{12} + 2B_{66})](-15 + \pi^2)}{b\pi^2}$$

$$a_4 = \frac{5a^3[b^2A_{22}(15 - 4\pi^2) + 3(A_{12} - A_{66})a^2(63 - 4\pi^2)]}{64b\pi^2}$$

$$a_5 = -abq_x$$

$$b_0 = \frac{ab^{11}}{18,480}\bar{m}, \qquad b' = \frac{a^{11}b}{18,480}d_2$$

$$b_1 = \frac{b^9(33a^2A_{22} + A_{66}b^2\pi^2)}{13,860a}$$

$$b_2 = \frac{a^5(A_{12} + A_{66})b^5(-15 + \pi^2)^2}{4\pi^8}$$

$$b_3 = -\frac{b^3[3a^2B_{22} + b^2(B_{12} + 2B_{66})](-15 + \pi^2)}{a\pi^2}$$

$$b_4 = \frac{5b^3[a^2A_{22}(15 - 4\pi^2) + 3(A_{12} - A_{66})b^2(63 - 4\pi^2)]}{64a\pi^2}$$

$$b_5 = -abq_y$$

$$c_0 = \frac{9ab}{4}\bar{m}, \qquad c' = \frac{9ab}{4}d_3$$

$$c_1 = \frac{4\pi^4[3b^4D_{11} + 3a^4D_{22} + 2a^2b^2(D_{12} + 2D_{66})]}{a^3b^3}$$

$$c_2 = \frac{24\pi^4}{ab}(B_{12} - B_{66})$$

$$c_3 = \frac{20\pi^4[21a^4A_{22} + 10a^2(3A_{12} + 4A_{66})b^2 + 21A_{11}b^4]}{32a^3b^3}$$

$$c_4 = -\frac{a^3[3b^2B_{11} + a^2(B_{12} + 2B_{66})](-15 + \pi^2)}{b\pi^2}$$

$$c_5 = -\frac{b^3[3a^2B_{22} + b^2(B_{12} + 2B_{66})](-15 + \pi^2)}{a\pi^2}$$

$$c_6 = \frac{5a^3[A_{11}b^2(15 - 4\pi^2) - 3a^2(A_{12} - A_{66})(-63 + 4\pi^2)]}{32b\pi^2}$$

$$c_7 = \frac{5b^3[A_{22}a^2(15 - 4\pi^2) - 3b^2(A_{12} - A_{66})(-63 + 4\pi^2)]}{32a\pi^2}$$

$$c_8 = -abP(t)$$

Coefficients in the finite difference equations:

$$A_1 = \frac{a_0}{(\Delta t)^2} + a_1 + \frac{a'}{\Delta t}, \qquad A_2 = a_2, \qquad A_3 = a_3 + a_4W^n$$

$$A_4 = \frac{a_0}{\Delta t}\dot{U}^n + \frac{a_0}{(\Delta t)^2}U^n + \frac{a'}{\Delta t}U^n - a_5$$

$$B_1 = b_2, \qquad B_2 = \frac{b_0}{(\Delta t)^2} + \frac{b'}{\Delta t} + b_1, \qquad B_3 = b_3 + b_4W^n$$

$$B_4 = \frac{b_0}{\Delta t}\dot{V}^n + \frac{b_0}{(\Delta t)^2}V^n + \frac{b'}{\Delta t}V^n - b_5$$

$$C_1 = c_4 + c_6W^n, \qquad C_2 = c_5 + c_7W^n$$

$$C_3 = \frac{c_0}{(\Delta t)^2} + c_1 + c_2W^n + c_3(W^n)^2 + \frac{c'}{\Delta t}$$

$$C_4 = \frac{c_0}{\Delta t}\dot{W}^n + \left(\frac{c_0}{(\Delta t)^2} + \frac{c'}{\Delta t}\right)W^n + c_8$$

$$D_1 = B_2 - \frac{B_1A_2}{A_1}, \qquad D_2 = B_3 - \frac{B_1A_3}{A_1}, \qquad D_3 = B_4 - \frac{B_1A_4}{A_1}$$

$$E_1 = C_2 - \frac{C_1A_2}{A_1}, \qquad E_2 = C_3 - \frac{C_1A_3}{A_1}, \qquad E_3 = C_4 - \frac{C_1A_4}{A_1}$$

$$E_4 = \frac{E_1D_3}{D_1}, \qquad E_5 = E_2 - \frac{E_1D_2}{D_1}$$

Acknowledgment

The authors wish to thank the T. R. Prime Ministry State Planning Organization for its support of the Project No. 901341998k121980 entitled "Investigation of explosion effects on structures."

References

[1] Leissa, A. W., "Vibration of Plates," NASA SP-160, Scientific and Technical Information Division, Office of Technology Utilization, NASA, Washington D.C., 1969.

[2] Reddy, J. N., "Geometrically Nonlinear Transient Analysis of Laminated Composite Plates," *AIAA Journal*, Vol. 21, No. 4, April 1983, pp. 621–629.

[3] Reddy, J. N., *Mechanics of Laminated Composite Plates: Theory and Analysis*, CRC Press, New York, 1997.

[4] Türkmen, H. S., and Mecitoğlu, Z., "Nonlinear Structural Response of Laminated Composite Plates Subjected to Blast Loading," *AIAA Journal*, Vol. 37, No. 12, Dec. 1999, pp. 1639–1647.

[5] Türkmen, H. S., and Mecitoğlu, Z., "Dynamic Response of a Stiffened Laminated Composite Plate Subjected to Blast Load," *Journal of Sound and Vibration*, Vol. 221, No. 3, 1999, pp. 371–389.

[6] Türkmen, H. S., "Structural Response of Laminated Composite Shells Subjected to Blast Loading: Comparison of Experimental and Theoretical Methods," *Journal of Sound and Vibration*, Vol. 249, No. 4, 2002, pp. 663–678.

[7] Nosier, A., Librescu, L., and Frederick, D., "The Effects of Time-Dependent Excitation on the Oscillatory Motion of Viscously Damped Laminated Composite Flat Panels," *Advances in the Theory of Plates and Shells*, edited by G. Z. Voyiadjis and D. Karamanlidis, Elsevier, Amsterdam, 1990, pp. 249–268.

[8] Librescu, L., Oh, S. Y., and Hohe, J., "Linear and Non-Linear Dynamic Response of Sandwich Panels to Blast Loading," *Composites, Part B: Engineering*, Vol. 35, Elsevier, New York, 2004, pp. 673–683.

[9] Kazancı, Z., Mecitoğlu, Z., and Hacıoğlu, A., "Effect of In-Plane Stiffnesses and Inertias on Dynamic Behavior of A Laminated Composite Plate Under Blast Load," *Proceedings of the 9th Biennial ASCE Aerospace Division International Conference on Engineering, Construction, and Operations in Challenging Environments, Earth & Space-2004*, ASCE Publications, Reston, VA, 2004, pp. 484–491.

[10] Rayleigh, J. W. S., *The Theory of Sound*, 2nd ed., Vols. 1, 2, 1894, reprinted by Dover Publications, New York, 1945.

[11] Weierstrass, K., "Über die Analytische Darstellbarkeit Sogenannter Willkürlicher Functionen Einer Reellen Veränderlichen," *Sitzungsberichte der Akademie zu Berlin*, 1885, pp. 633–639, 789–805; also appeared in Weierstrass' "Mathematische Werke," Mayer and Muller, Berlin, Vol. 3, 1903, pp. 1–37.

[12] Gupta A. D., Gregory F. H., Bitting, R. L., and Bhattacharya, S. "Dynamic Analysis of an Explosively Loaded Hinged Rectangular Plate," *Computers and Structures*, Vol. 26, No. 1–2, Aug. 1987, pp. 339–344.

[13] Strang G., *Introduction to Applied Mathematics*, Wellesley–Cambridge Press, Wellesley, MA, 1986.

K. Shivakumar
Associate Editor